The human plasma amino acids balance favours HIV replication in primary CD4 T lymphocytes

Lise Chauveau[1@], Annemarie Fortuin[1*], Arnaud Lecante[1*], Nina Lager-Lachaud[2,3], Angéline Tellier[1], Shravya Honne[4], Aude Boulay[5], Fabien P Blanchet[5], Baek Kim[4], Floriant Bellvert[2,3], Laurence Briant[1^@] and Jean-Luc Battini[1^@]

[1] RNA viruses and metabolism team, Institut de Recherche en Infectiologie de Montpellier, CNRS UMR 9004, Université de Montpellier, Montpellier, France.
[2] Toulouse Biotechnology Institute, Université de Toulouse, CNRS, INRA, INSA, Toulouse, France.
[3] MetaToul-MetaboHUB, National Infrastructure of Metabolomics and Fluxomics, Toulouse, France.
[4] Center for ViroScience and Cure, Department of Pediatrics, School of Medicine, Emory University, Atlanta, Georgia, USA.
[5] Quantitative Biology of Membrane Traffic and Pathogenesis team, Institut de Recherche en Infectiologie de Montpellier, CNRS UMR 9004, Université de Montpellier, Montpellier, France.

* Contributed equally to this work
^ Co-last authors
[@] Corresponding authors: lise.chauveau@cnrs.fr, Laurence.briant@irim.cnrs.fr, jean-luc.battini@irim.cnrs.fr

Abstract

Cellular metabolism supports all viral replication steps and the metabolic state of infected cells is therefore a key factor influencing viral infections. Human Immunodeficiency virus (HIV) remains latent in resting CD4 T lymphocytes but actively replicates in activated CD4 T cells due to enhanced energy metabolism. Here, using the recently developed Human Plasma-Like Medium (HPLM) that mimics physiological plasma concentration of metabolites, we investigated how this near-physiologic environment modulates HIV-1 infection in primary CD4 T cells. Compared to the conventional culture medium (RPMI), HPLM enhanced HIV-1 infection in CD4 T cells despite similar levels of cell activation, proliferation and expression of viral receptor. In contrast with previous studies in RPMI, HPLM increased infection while decreasing energy metabolism and affecting other non-energetic metabolic pathways. Adjusting levels of several metabolites in RPMI and HPLM, we uncovered that the amino acids balance rather than the energy metabolism favoured HIV-1 replication in this system. Overall, our study used near-physiological conditions to better define metabolic dependencies of viral infections and highlights previously overlooked non-energetic metabolism pathways important for HIV-1 infection.

Introduction

The Human Immunodeficiency Virus (HIV) is responsible for the worldwide pandemic of Acquired ImmunoDeficiency Syndrome (AIDS). Since the start of the pandemic, 40 years ago, HIV has infected an estimated 88.4 million patients and killed 42.3 million. In 2023, 39.9 million people were still living with HIV[1]. With the development of antiretroviral therapy, AIDS has become a manageable lifelong condition[2] but no cure or vaccine currently exist[3]. Increasing our understanding of the interaction between HIV-1 and its cellular targets in physiological conditions is crucial to propose better suited treatments.

Cellular metabolism encompasses all pathways involved in the generation or recycling of biomolecules used for energy production, nucleic acid or protein synthesis, regulation of gene expression, redox balance and many other cellular processes. All molecules involved are called metabolites and their homeostasis is tightly regulated. The two main pathways producing energy in the form of ATP are glycolysis and mitochondrial respiration (OXPHOS). HIV-1 mainly infects CD4 T lymphocytes, immune cells crucial for establishing pathogen-specific adaptive immune responses. Upon recognition of pathogen-derived antigens, CD4 T cells are activated and shift from naïve resting cells to actively dividing cells producing large amounts of cytokines. Thus, while naïve T cells keep a low energy supply using low levels of glycolysis and OXPHOS[4], activated CD4 T cells undergo a profound metabolic reprogramming to meet higher metabolic demands. Increased glucose uptake leads to higher rates of glycolysis to produce energy. Moreover, intermediates in the glycolysis pathway are diverted into other pathways such as the pentose phosphate pathway (PPP) to produce deoxynucleotide triphosphates (dNTPs) and amino acids essential for the cells' immune functions.

The HIV-1 replication cycle is initiated by the interaction of the viral particle with its receptor (CD4) and co-receptors (CXCR4 or CCR5), leading to the fusion of viral and cellular membranes. Following entry in the cytoplasm, the viral RNA genome is reverse transcribed into a proviral DNA that is imported in the nucleus and integrated in the host genome. From there, viral genes are transcribed and viral proteins are produced which leads to assembly of new viral particles and their budding from the plasma membrane. The different steps of the viral life cycle therefore require the availability of specific metabolites. The increased glycolysis occurring during CD4 T cell activation is associated with higher susceptibility to HIV-1 infection[5–9]. Recent studies even showed that HIV-1 preferentially infects cells with high glycolytic activity, irrespective of their activation status, and blocking glycolysis prevents infection of primary CD4 T cells[7,10]. Both glycolysis and glutaminolysis, which uses glutamine as a carbon source to feed OXPHOS, are essential for HIV-1 replication in these cells[11].

However, most of these studies were performed *in vitro* using the standard, but not physiologic, RPMI-1640 cell culture medium that was formulated to sustain cell proliferation[12]. Therefore, more physiologically relevant cell culture conditions are needed. Recently, new cell culture media were developed, such as the Human Plasma-Like Medium (HPLM) that closely mimics the metabolite composition of human plasma[13]. Unlike RPMI, HPLM contains 31 polar metabolites absent from commonly used media and carries other components such as

80 glucose, glutamine and amino acids at physiological concentrations. HPLM shapes the immune
81 response in CD4 T cells by influencing the metabolic state of the cells[14,15].
82 Here, we investigated how the human plasma metabolic environment affects HIV-1 replication
83 in primary activated CD4 T cells *in vitro*. Compared to RPMI, we found that HPLM potentiated
84 HIV-1 replication by increasing the viral reverse transcription. In contrast with the previous
85 reports performed in RPMI, this increase was associated with lower energy metabolism and
86 lower glycolysis. However, adjusting glucose and glutamine levels in RPMI to match HPLM or
87 inhibiting the energy metabolism using chemical inhibitors did not recapitulate the increased
88 infection observed in HPLM. Instead, adjusting amino acids concentrations in RPMI and HPLM
89 resulted in a similar intermediate infection rate, suggesting that the balance of amino acids in
90 physiological conditions is optimal for HIV-1 replication. Our results therefore highlight the
91 importance of other metabolic pathways that are key for HIV-1 replication in these new near-
92 physiological conditions and were previously overlooked.
93
94 **Results**
95 Human plasma-like metabolic environment potentiates HIV-1 replication in primary activated
96 CD4 T cells
97 We first wondered if the human plasma-like metabolic environment would affect HIV-1
98 replication in primary CD4 T cells. CD4 T cells activated in RPMI or in HPLM showed a similar
99 activation by flow cytometry monitoring the activation marker CD25 and cell divisions using
100 Cell Trace (Fig 1A and B). Activated cells were then infected with two doses of HIV-1 NL4-3
101 virus and virus replication was monitored by flow cytometry looking at expression of the viral
102 Gag protein 4 days post-infection (dpi). Cells cultured in HPLM showed a significantly higher
103 HIV-1 replication compared to those cultured in RPMI with a 2- to 5-fold increase depending
104 on the viral dose used (Fig 1C and D). Treatment with the non-nucleoside reverse transcriptase
105 inhibitor nevirapine (NVP) confirmed that the observed fluorescence correlated with HIV-1
106 replication (Fig 1C and D). Time course experiments further showed that this increase was not
107 merely due to differences in kinetics of viral replication but to an increased proportion of cells
108 getting actively infected with infection rates reaching up to 65% in HPLM (Fig 1E).
109 To confirm the physiological relevance of our results, we next used the transmitted-founder
110 virus HIV-1 WITO as well as 3 primary viral isolates from treatment-naïve patients with high
111 viral loads (patients 4, 15 and 17)[16]. We infected CD4 T cells activated in RPMI or HPLM with
112 these viruses and observed a similar increase in replication (Fig 1F and G) with a 3-fold increase
113 in HIV-1 WITO infection and fold changes ranging from 2 to 7 for the primary isolates revealing
114 variability between donors of the cells used for the infection.
115 Therefore, HPLM potentiates the replication of several HIV-1 strains including primary isolates
116 in primary activated CD4 T cells.
117
118 HPLM enhances HIV-1 reverse transcription
119 To investigate the viral replication step affected by the medium, we successively assessed
120 several steps of the viral life cycle using the well-characterised HIV-1 NL4-3 strain. First, we

121 observed that cell surface expression of the HIV-1 receptor (CD4) and co-receptors (CXCR4
122 and CCR5) were similar when CD4 T cells were activated in each medium (Fig 2A). We then
123 evaluated viral binding by incubating activated CD4 T cells with HIV-1 NL4-3 at 4°C to only
124 allow binding of the HIV-1 viral particle at the cell surface. Quantification of bound particles
125 by HIV-1 Gag p24 ELISA showed no difference between the two media (Fig 2B). Next, we tested
126 if virus fusion at the plasma membrane was affected using the Vpr-Blam assay[17]. Briefly, Vpr,
127 an HIV-1 protein incorporated into the viral particles, is fused with the beta-lactamase (Vpr-
128 Blam). Cells are pre-loaded with CCF2-AM, a cell-permeable fluorescent substrate of beta-
129 lactamase, and infected with viral particles containing Vpr-blam. Upon virus fusion, Vpr-Blam
130 is delivered to the cytosol where it cleaves CCF2-AM, triggering a fluorescent switch quantified
131 by flow cytometry. Using two different doses of HIV-1 NL4-3 Vpr-Blam, we did not observe
132 any difference in fusion between the two media (Fig 2C). We next evaluated reverse
133 transcription (RT) of HIV-1 RNA into DNA, which can be quantified by qPCR using primers
134 specific for the amplification of early and late RT products. CD4 T cells were infected for 18h
135 in the presence or not of the RT inhibitor NVP. We quantified RT products by qPCR on
136 normalised amounts of cellular DNA and calculated copy numbers of early and late RT
137 products using a plasmid standard. We observed a significant 4-fold increase in both early and
138 late RT products in cells cultured in HPLM, suggesting that RT activity is increased in HPLM
139 conditions (Fig 2D).
140 To assess HPLM effects on the late phases of the HIV-1 life cycle, we quantified virus particle
141 released in the supernatant of infected cells by HIV-1 Gag p24 ELISA. Concentration of virus
142 particles were significantly increased in the supernatant of cells infected in HPLM at 4 dpi,
143 correlating with the increased percentage of infected cells in this condition (Fig 2E). However,
144 the infectivity of the virus particles produced assessed on the TZM-bl reporter cell line showed
145 a non-significant decrease (Fig 2F) suggesting that the increased virus particle production
146 could compensate a decrease in particle infectivity.
147 Therefore, HPLM potentiates HIV-1 replication in activated CD4 T cells primarily by increasing
148 the RT step of the viral life cycle.
149
150 <u>HPLM affects cellular metabolism of primary activated CD4 T cells</u>
151 HPLM and RPMI formulations differ in the concentrations of three groups of metabolites:
152 carbon sources essential for energy production (glucose, 5mM vs 11mM in RPMI; glutamine,
153 0.55mM vs 2mM in RPMI); amino acids; and other polar metabolites including some involved
154 in the TCA cycle used in energy metabolism[13]. To investigate how these differences affect CD4
155 T cells metabolism, we analysed energy metabolism in cells activated in HPLM or RPMI using
156 the ATP rate assay with the Seahorse technology. This method measures the oxygen
157 consumption linked to OXPHOS, and the medium acidification due to lactate export following
158 glycolysis in live cells. It then calculates the overall ATP production rate and distinguishes ATP
159 produced by glycolysis (glycoATP) and by OXPHOS (mitoATP). Activated CD4 T cells had a lower
160 overall ATP production rate and significantly lower glycolysis in HPLM vs RPMI (Fig 3A). We
161 further analysed the metabolism of CD4 T cells activated in HPLM or RPMI by metabolomics

162 using high-resolution mass spectrometry (HRMS). We monitored central metabolism and
163 amino acids by ion chromatography coupled HRMS (IC-HRMS) and liquid chromatography
164 coupled HRMS (LC-HRMS) respectively. PCA analysis indicated significant metabolic
165 differences between the two conditions (Fig 3B). Volcano plot analysis revealed significantly
166 different metabolites (both fold change >2 and p-value<0.1; Fig 3C). Heatmaps for each group
167 of metabolites confidently identified showed specific metabolites variations (Fig 3D). A few
168 metabolites were significantly more abundant in HPLM-activated cells, including
169 phosphorybosyl-pyrophosphate (PRPP), a key metabolite in the pentose phosphate pathway
170 (PPP), and multiple pentose-5-phosphate metabolites, suggesting that the PPP is upregulated
171 in HPLM-activated cells. Moreover, histidine, threonine, glycine, valine, phenylalanine and
172 tyrosine were also elevated in HPLM. Interestingly, this increase did not correlate with higher
173 concentrations of histidine, threonine, phenylalanine and tyrosine in the HPLM medium. In
174 contrast, 21 metabolites were significantly more abundant in RPMI-activated cells, including
175 (i) glutamine and glucose-6-phosphate, the main form of glucose present in cells, reflecting
176 the higher concentrations of these carbon sources in RPMI; (ii) intermediates of glycolysis; (iii)
177 intermediates of the TCA cycle; (iv) intermediates of the hexosamine pathway; and (v) amino
178 acids, mostly reflecting differences in the culture media. We found above that HPLM increases
179 the HIV-1 RT that heavily relies on dNTPs. Specific quantification of cellular dNTPs revealed a
180 decrease in dATP and dTTP and no changes in dCTP or dGTP in HPLM-activated cells (Fig 3E),
181 suggesting that the levels of dNTPs are still sufficient to support RT and are not involved in the
182 phenotype observed.
183 Overall, these results, summarised in Fig 3F, show that all energy metabolism pathways are
184 down-regulated in cells activated in HPLM, while other metabolic processes such as amino
185 acids and nucleotides metabolisms, the PPP and the hexosamine pathway are altered.
186
187 <u>HPLM enhances HIV-1 infection by providing an optimal amino acid balance</u>
188 Previous studies have demonstrated that glycolysis and glutaminolysis are crucial for HIV-1
189 replication in CD4 T cells activated in RPMI[10,11]. However, HPLM has lower concentrations of
190 glucose and glutamine leading to lower energy metabolism but, paradoxically, HIV-1 replicates
191 more efficiently. We hypothesised that lower but physiological concentrations of glucose and
192 glutamine in HPLM could favour HIV-1 replication. We used RPMI without glucose and
193 glutamine supplemented with 5mM glucose and 0.55mM glutamine to match the physiologic
194 concentrations in HPLM (RPMI+Carb). Seahorse analysis showed that cells activated in
195 RPMI+Carb had an intermediate metabolic phenotype that was not significantly different from
196 either RPMI or HPLM (Fig 4A). However, HIV-1 replication in cells activated in RPMI+Carb was
197 similar to RPMI and significantly lower than in HPLM at the two viral doses tested (Fig 4B).
198 Thus, the different energy metabolism in HPLM-activated cells is not linked to the enhanced
199 HIV-1 replication. To confirm that HIV-1 replication still relies on energy metabolism in HPLM,
200 we used three chemical inhibitors targeting different steps in these pathways (summarised in
201 Fig 4C): 2-deoxyglucose (2-DG) targets hexokinase the first rate-limiting enzyme of glycolysis;
202 sodium fluoroacetate (NaFlAc) targets Aconitase and inhibits the TCA cycle shortly after entry

203 of the products of glycolysis; and dimethyl-malonate (DMM) inhibits succinate
204 dehydrogenase, also known as complex II of the mitochondrial respiration chain, the key
205 enzyme to use TCA metabolites in OXPHOS. CD4 T cells activated in RPMI or HPLM were
206 infected with HIV-1 NL4-3 in the presence of these inhibitors. Regardless of the culture
207 medium used, HIV-1 replication was blocked by treatment with 2-DG with an even more
208 pronounced effect in HPLM than in RPMI (Fig 4D). The TCA inhibitors had no significant effect
209 on viral replication with only DMM inducing a non-significant decrease in HIV-1 replication in
210 RPMI.
211 Our metabolomics analysis also revealed a significant difference in the amino acid balance in
212 cells activated in HPLM vs RPMI. We compared the concentrations of all amino acids in the
213 HPLM and RPMI media and identified 4 amino acids with higher concentrations in HPLM and
214 13 amino acids higher in RPMI (Fig 4E). We therefore adjusted the concentrations of each
215 group of amino acids by adding the 4 in RPMI (RPMI+all AA) and adding the 13 in HPLM
216 (HPLM+all AA). CD4 T cells activated and infected in these media showed an intermediate
217 infection rate that was no longer significantly different between RPMI+all AA and HPLM+all
218 AA (Fig 4F). Fold changes compared to their respective unmodified media revealed that
219 adjusting the amino acids concentrations in RPMI resulted in a 1-to-6-fold increase in HIV-1
220 replication depending on the donors, while adjusting the amino acids concentrations in HPLM
221 resulted in a 2-fold decrease in HIV-1 replication.
222 Therefore, while the low glycolysis observed in CD4 T cells activated in HPLM is still crucial for
223 HIV-1 infection, it is not the differences in energy metabolism between RPMI and HPLM but
224 rather the amino acids balance that is involved in the increased HIV-1 replication in cells
225 cultured in HPLM.
226
227 **Discussion**
228 In this study, we interrogated the impact of the human plasma metabolic environment on HIV-
229 1 replication in primary activated CD4 T cells. Taking advantage of the recently formulated
230 HPLM as a near-physiologic medium and comparing it to the standard RPMI medium, we show
231 that CD4 T cells activated in HPLM are significantly more susceptible to infection by several
232 strains of HIV-1, including primary isolates from patients. In particular, HPLM increased the
233 reverse transcription (RT) step of the viral replication cycle. Surprisingly, and in contrast to
234 previous studies performed in RPMI, the enhanced HIV-1 replication was associated with a
235 lower energy metabolism, and in particular a lower glycolysis. Several metabolic pathways
236 were affected by the use of HPLM including the Pentose Phosphate Pathway (PPP), the
237 hexosamine pathway and intracellular concentrations of dNTPs and amino acids. The low
238 glycolysis in HPLM-cultured cells was still crucial for HIV-1 infection. However, we show that
239 the optimal amino acids balance in HPLM, rather than the energy metabolism, is responsible
240 for the increased HIV-1 replication in these near-physiological conditions.
241 HPLM potentiated the replication of several HIV-1 strains including primary isolates from
242 treatment-naïve patients extending our findings to the most physiologically-relevant
243 replication-competent viruses. This increased replication was observed in cells showing similar

244 cellular activation or proliferation. The kinetics of replication in our assays were also similar
245 between the two media with the peak of infection reaching up to 65% in HPLM vs 45% in RPMI
246 suggesting that it is the number of cells susceptible to infection that was increased in HPLM.
247 These results are concordant with previous findings showing that CD4 T cells proliferation[7] or
248 activation[10] status do not predict susceptibility to HIV-1 infection. Instead, the former study
249 found that the metabolic state of the cells, and in particular their uptake of glucose, is
250 important for HIV-1 RT. Similarly, we observed a 3-fold increase in HIV-1 RT at 18 hours post-
251 infection in HPLM-activated CD4 T cells, which likely contributed to the increased viral
252 replication observed at 4 days post-infection. The RT step of the viral life cycle is highly
253 dependent on cellular metabolism which conditions availability of the necessary dNTPs[18]. Our
254 metabolomics analysis revealed an increased PPP in HPLM-cultured cells and this pathway
255 provides precursors for *de novo* dNTPs synthesis. However, our intracellular dNTPs
256 quantification unexpectedly revealed decreased dNTPs concentrations in HPLM-cultured cells,
257 particularly dTTP and dATP. HPLM was previously shown to inhibit *de novo* pyrimidine
258 synthesis in cancer cell lines by providing urea, a specific inhibitor of this pathway[13]. In primary
259 CD4 T cells, HPLM could therefore both increase the PPP and block dTTP and dATP synthesis
260 via unknown mechanisms worth exploring in the future. Our results show that this lower
261 concentration of dNTPs is still sufficient to support HIV-1 RT in HPLM-activated CD4 T cells and
262 suggest that other metabolites modulated by HPLM are important for HIV-1 RT. Moreover,
263 whether this result reflects more RT per infected cell or an increase in the number of cells
264 where the RT step is efficient could not be determined in our assays. We can also not exclude
265 that another unexamined step of the viral replication cycle, such as integration of the viral
266 genome or cell-to-cell viral transmission, may contribute to the increased HIV-1 replication in
267 HPLM conditions.
268 HPLM decreases the hexosamine pathway while increasing the PPP in activated CD4 T cells.
269 The hexosamine pathway produces UDP-N-acetyl-D-glucosamine (UDP-GlcNAc), the substrate
270 for both N- and O- protein glycosylations, and is therefore important for this protein post-
271 translational modification. In the context of HIV-1 infection, glycosylation of the Sp1
272 transcription factor was shown to inhibit HIV-1 transcription from the LTR both in T cell lines
273 and in primary CD4 T cells[19]. In HPLM, the decreased hexosamine pathway could therefore
274 decrease Sp1 glycosylation and increase HIV-1 transcription. The HIV-1 envelope gp120 is also
275 glycosylated which increases viral particle infectivity while decreasing recognition by
276 neutralising antibodies[20]. In HPLM, this could explain the trend of decreased viral particles
277 infectivity observed in Fig 2F which warrants further investigations. As previously mentioned,
278 the PPP provides precursors for nucleotides synthesis but also precursors for amino acids
279 synthesis, and NADPH for oxidative stress management. While we show that nucleotide levels
280 are unaffected or decreased in HPLM, other downstream effects of the increased PPP in HPLM
281 could be involved in the enhanced HIV-1 replication. Interestingly, the metabolic phenotype
282 we observe in HPLM – downregulated glycolysis with increased PPP activity - is a hallmark of
283 the establishment of HIV-1 latency[21]. HPLM could therefore serve as a valuable model for

284 studying HIV-1 latency, the current main hurdle in the search for an HIV cure, and exploring
285 therapeutic strategies such as “shock and kill”.
286 Glycolysis and OXPHOS are key pathways previously shown to support HIV-1 infection in CD4
287 T cells activated in RPMI [10,11,22]. Inhibitors of these pathways were reported to significantly
288 reduce HIV-1 infection[10]. However, despite exhibiting lower energy metabolism, CD4 T cells
289 activated in HPLM showed a higher susceptibility to HIV-1 infection. Our findings reveal that
290 decreased energy metabolism is not directly responsible for the increased infection, as
291 adjusting glucose and glutamine levels in RPMI to match HPLM did increase HIV-1 replication
292 to levels found in HPLM-activated CD4 T cells. In line with previous reports, we show that the
293 glycolysis inhibitor 2-DG decreased HIV-1 replication, with an even more pronounced effect in
294 HPLM than in RPMI. Our results therefore extend these previous findings to CD4 T cells
295 cultured in HPLM where the limited glucose availability might increase 2-DG efficacy. In
296 contrast, we did not observe a significant effect with TCA cycle or OXPHOS inhibitors such as
297 DMM that lead to a non-significant decrease in HIV-1 replication in RPMI and only a modest
298 effect in HPLM. This result contradicts recent studies[22] and suggests that HIV-1’s reliance on
299 OXPHOS might differ between the two media.
300 Amino acids are another group of metabolites that are present at different concentrations in
301 HPLM and in RPMI. Our metabolomics analysis revealed that amino acids metabolism was
302 differentially regulated in cells activated in each medium suggesting that they could be of
303 importance for HIV-1 replication. When adjusting the concentrations of amino acids, adding
304 some in RPMI and others in HPLM, we observed an intermediate infection rate that was similar
305 between the two adjusted medium. Therefore, amino acids that we added into RPMI could
306 have pro-viral effects and amino acids added into HPLM could have anti-viral effects. Some of
307 the amino acids in both lists already have pro- or antiviral effects described in the context of
308 HIV-1 infection. For instance, tryptophane present in HPLM enhances HIV-1 transcription in
309 cell lines and viral reactivation in latently infected cells derived from people living with HIV[23].
310 Moreover, arginine present in RPMI can be used to produce polyamines that have an antiviral
311 role by blocking HIV-1 fusion[24]. The effects of individual amino acids and their combinations
312 on HIV-1 replication in the context of HPLM requires further investigation.
313
314 In conclusion, our study identifies the amino acid balance in human plasma as a crucial factor
315 favouring HIV-1 replication in primary CD4 T cells. It further highlights the critical role of
316 metabolic pathways other than glycolysis and OXPHOS that have been overlooked in this
317 context and will deserve attention in the future to identify new therapeutic targets. We also
318 argue for the importance of using physiologically relevant models, which encompasses
319 primary cells and more physiologic culture media, to investigate host-pathogen interactions,
320 especially when looking at metabolic dependencies. This needs to be particularly considered
321 for antiviral drugs development and for the study of latent HIV-1-infected CD4 T cells which
322 account for HIV-1 persistence and incurable life-long infection in people living with HIV.

323 **Materials and methods**

324 **Cells**

325 Cells were kept in culture in the following media: classical RPMI-1640 medium (Gibco); newly
326 developed Human Plasma-Like Medium (HPLM, Gibco); RPMI without glucose and glutamine
327 (PAN Biotech) where glucose was added at 5mM and glutamine at 0.55 mM to match the
328 concentrations in HPLM (RPMI+Carb); RPMI (Gibco) complemented with various amino acids
329 to match the concentrations in HPLM (RPMI+all AA); or HPLM (Gibco) complemented with
330 various amino acids to match the concentrations in RPMI (HPLM+all AA). RPMI, RPMI+Carb
331 and RPMI+all AA were supplemented with 10% heat-inactivated fetal calf serum (FCS) and 1%
332 PenStrep (Gibco). HPLM and HPLM+all AA were supplemented with 10% heat-inactivated
333 dialysed FCS (Gibco) and 1% PenStrep (Gibco).
334 PBMCs were isolated from the blood of healthy donors by Ficoll centrifugation. The blood was
335 provided by the EFS (Etablissement Francais du Sang, the official French blood bank). CD4+ T
336 lymphocytes were isolated from PBMCs by positive selection using magnetic beads (EasySep
337 Human CD4 positive selection kit II, StemCell Technologies) and activated using ImmunoCult
338 human CD3/CD28 T cell activator cocktail (StemCell Technologies) then grown in the indicated
339 medium in presence of 100U/mL IL-2 (StemCell Technologies) for 4 days before being used in
340 the various experiments. In all experiments, IL-2 was added in the culture medium at a final
341 concentration of 100U/mL to support cell survival and growth.
342 HEK293T and TZM-bl cells were cultured in DMEM supplemented with 10% FCS and 1%
343 PenStrep (Gibco).
344

345 **Reagents**

346 The reverse transcription inhibitor nevirapine (NVP) was from the NIH AIDS reagents program.
347 The following metabolic inhibitors were used: 2-deoxy-glucose (2-DG, 5mM; Sigma); dimethyl
348 malonate (DMM, 10mM; Sigma); sodium fluoroacetate (NaFlAc, 10μM; CliniSciences).
349

350 **Viruses**

351 HIV-1 NL4-3 and WITO were generated by transfection of pNL4-3 and pWITO.c/2474,
352 respectively, in HEK293T cells. Briefly, HEK293T cells were seeded in T175 flasks and
353 transfected the next day using PEIpro (Polyplus). After overnight incubation, the medium was
354 changed and the supernatant was collected 24h, 32h and 48h later. The three harvests were
355 pooled and concentrated by ultracentrifugation through a 20% sucrose cushion at 100,000g
356 for 2h then resuspended in PBS. Primary isolates from treatment-naïve patients were a kind
357 gift from Nathalie Arhel and have been previously described[16]. The concentration of the viral
358 stock was determined using HIV-1 Gag p24 ELISA (Lenti-X™ p24 Rapid Titer Kit #631476,
359 Takara; or Innotest HIV Ag mAb, Fujirebio). The doses used in all experiments were chosen by
360 infecting primary CD4 T cells to reach appropriate levels of infection and were adjusted for
361 each viral production.
362

363 **HIV-1 infection**

364 150 000 primary CD4 T cells were seeded in round-bottom 96-well plates and infected in a
365 final volume of 100uL with 10, 25, 40 or 200 ng p24/mL of HIV-1 NL4-3 WT as indicated, or
366 900ng p24/mL HIV-1 WITO, or viruses from patients at the indicated concentrations. When
367 indicated, the reverse transcriptase inhibitor NVP or the metabolic inhibitors were added in
368 the wells at the time of infection.
369 For analysis of HIV-1 reverse transcription, the input virus was first treated with RQ1 DNase
370 (Promega) for 1h at 37°C before adding to the cells to remove left-over plasmid from the
371 production transfection. Two hours after infection, the cells were washed in PBS to remove
372 input virus and kept in culture for an additional 18h.
373 For analysis of the virus particle release in the supernatant, the cells were washed twice in PBS
374 2h after infection in order to remove the input virus and kept in culture for 3 or 4 days.
375
376 **Flow cytometry**
377 To assess activation of the CD4 T cells prior to infection, activated cells were stained with anti-
378 CD25 FITC (Biolegend) in PBS+2%FCS+1mM EDTA (FACS Buffer) for 30min at 4°C and washed
379 twice in FACS Buffer.
380 To quantify proliferation of the CD4 T cells, cells were stained directly after isolation from
381 PBMCs with the CellTrace Far Red (ThermoFischer Scientific) in PBS for 20min at 37°C. Medium
382 was added to the cells to dilute the dye and further incubated for 5min at RT. Cells were then
383 centrifuged, resuspended in the appropriate volume of each medium and activated with the
384 ImmunoCult activation cocktail. Proliferation was monitored by flow cytometry at day 5 post-
385 activation by looking at loss of fluorescence due to cell division and the percentage of cells
386 having divided at least once was calculated.
387 To assess the infection rate at the indicated days post-infection, cells were stained with a
388 fixable viability dye (LIVE/DEAD fixable far red viability stain, ThermoFisher Scientific) and fixed
389 in 4% PFA for 15min at room temperature. Intracellular Gag staining was performed by
390 permeabilising cells in FACS Buffer + 0.5% Triton X-100 for 20min at RT then staining with the
391 FITC-conjugated KC-57 anti-Gag antibody (Beckman-Coulter) in FACS Buffer for 30min at 4°C.
392 After two washes in FACS buffer, the infection was analysed by flow cytometry looking at the
393 percentage of cells expressing Gag.
394 All samples were analysed with a NovoCyte Flow Cytometer (Agilent).
395
396 **Binding assay**
397 150 000 primary CD4 T cells were seeded in round-bottom 96-well plates and placed at 4°C
398 for 2h. They were then incubated with 200ng p24/mL HIV-1 NL4-3 for 30min at 4°C. Unbound
399 viral particles were washed 4 times in PBS, cells were lysed and bound viral particles were
400 quantified using HIV-1 Gag p24 ELISA (Innotest HIV Ag mAb, Fujirebio) according to
401 manufacturer's instructions.
402
403 **Fusion assay**

404 Viral fusion was assessed as previously described[17]. Briefly, ultracentrifuged HIV-1 NL4-3
405 virions containing the Blam-Vpr fusion protein (a kind gift from Caroline Goujon) were used to
406 infect primary CD4 T cells. After 2h, cells were washed in CO_2-independent medium
407 supplemented with 10% FCS then incubated in CCF2-AM loading solution (CCF2-AM kit,
408 ThermoFisher scientific) containing 2.5mM Probenecid (Sigma) for 2h at room temperature.
409 Cells were then washed in CO_2-independent medium supplemented with 10% FCS and 2.5mM
410 Probenicid and further incubated overnight in the same medium. The next day, cells were
411 washed with PBS, fixed in 4% PFA for 15min, resuspended in FACS Buffer and analysed with a
412 Novocyte Flow Cytometer looking at CCF2-AM in the AmCyan channel and cleaved CCF2-AM
413 in the Violet channel.
414
415 **Reverse transcription assay**
416 Infected cells DNA was extracted using the DNeasy Blood and Tissue kit (Qiagen). Between 50-
417 100ng of total DNA were used with the LightCycler 480 SYBR Green I Master mix (Roche) and
418 amplified on a BioRad CFX Opus 384 Real-time PCR system. Primers for HIV-1 NL4-3 ssDNA
419 early products were: M667 (5'- GGCTAACTAGGGAACCCACTG -3') and AA55M (5'-
420 GCTAGAGATTTTCCACACTGACTAA -3') and for strand transfer late products: M667 and M661
421 (5'- CCTGCGTCGAGAGAGCTCCTCTGG -3'). PCR conditions were as follows: 95°C for 10min then
422 40 cycles of 95°C 15s, 65°C 15s and 70°C 20s. Quantities of cellular DNA were calculated using
423 a plasmid standard and normalised to the amount of DNA used.
424
425 **Virus particle release assay**
426 At days 3 and 4 post-infection, supernatant of infected cells was harvested after cell
427 centrifugation and frozen at -80°C. p24 titration was performed using an HIV-1 Gag p24 ELISA
428 kit according to the manufacturer's protocol (Lenti-X™ p24 Rapid Titer Kit #631476, Takara; or
429 Innotest HIV Ag mAb, Fujirebio).
430
431 **Viral particle infectivity assay**
432 Infectivity of the viral particles found in cell supernatants and quantified as described above
433 was assessed on the TZM-bl reporter cell line that expresses Luciferase under the HIV-1 LTR
434 promoter. 10 000 TZM-bl cells were seeded in flat-bottom 96-well plates. The next day,
435 medium was changed and 5ng p24 of each supernatant was added to the cells in duplicate.
436 48h post-infection, cells were lysed in Passive Lysis Buffer (Promega) and Firefly Luciferase
437 activity was quantified using Genofax A (Yelen).
438
439 **Seahorse ATP rate assay**
440 Seahorse analyses of the energy metabolism in activated CD4 T cells were performed using
441 the ATP rate assay (Seahorse Biosciences, Agilent) following manufacturer's protocol. Briefly,
442 cells were counted, resuspended in Seahorse RPMI culture medium and seeded in six
443 replicates in XF96 plates pre-coated with 0.1mg/mL poly-D-lysine. Cells were then incubated
444 for a minimum of 1h in a CO_2-free incubator at 37°C before the plate was loaded in the

445 Seahorse XF96e analyser. The protocol for the ATP rate assay was used following
446 manufacturer's instructions with the following injections: (1) oligomycin (1μM); and (2)
447 rotenone and antimycin A (1μM each) in ports A and B respectively. The ATP rate assay
448 analysis was performed using the Seahorse Analytics online software.
449
450 **Metabolomics analyses by IC- and LC-HRMS**
451 For metabolomics analyses, CD4 T cells were activated in RPMI or HPLM for 5 days then
452 washed in cold PBS and cell pellets were snap-frozen in liquid nitrogen and stored at -80°C
453 until metabolites extraction. Sampling buffer (acetonitrile:methanol:water at a ratio of 4:4:2
454 + 1.25mM formic acid) was prepared and cooled to -20°C 2h before extraction. Cell pellets
455 were resuspended in 1mL sampling buffer with IDMS controls and incubated for 1h at -20°C.
456 Cell debris were discarded by centrifugation at 2000g for 5min at 4°C. Supernatants containing
457 metabolites were transferred into a new tube, dried using a Speedvac and stored at -80°C until
458 mass spectrometry analyses.
459 Central metabolites were separated on an ionic chromatography column IonPac AS11 (250 ×
460 2 mm i.d.; Dionex, CA, USA). Mobile phase used was a gradient of KOH at a flow rate of 380
461 µL/min. Mobile phase was varied as follows: 0 min: 7 mM, 1 min: 7 mM, 9.5 min: 15 mM, 20
462 min: 15mM, 30 min: 45 mM, 33 min: 70mM, 33.1 min: 100mM and 42 min: 100mM. The
463 column was then equilibrated for 5 min at the initial conditions before the next sample was
464 analyzed. Time of analysis is 50 minutes. The volume of injection was 15µL. High-resolution
465 experiments were performed with an ICS5000+, ion chromatography system (Dionex, CA,
466 USA) system coupled to an Orbitrap Qexactive+ mass spectrometer (Thermo Fisher Scientific,
467 Waltham, MA, USA) equipped with a heated electrospray ionization probe. MS analyses were
468 performed in negative FTMS mode at a resolution of 70 000 (at 400 m/z) in full-scan mode,
469 with the following source parameters: the capillary temperature was 350 °C, the source heater
470 temperature, 350 °C, the sheath gas flow rate, 50 a.u. (arbitrary unit), the auxiliary gas flow
471 rate, 10 a.u., the S-Lens RF level, 65 %, and the source voltage, 2.75 kV. Metabolites were
472 determined by extracting the exact mass with a tolerance of 5 ppm.
473 For amino acid analysis, amino acids were separated on a PFP column (150 x 2.1 mm i.d.,
474 particle size 5 μm; Supelco Bellefonte, PEN, USA). Solvent 1 was 0.1% formic acid in H2O and
475 solvent B was 0.1% formic acid in acetonitrile at a flow rate of 250 mL/min. The gradient was
476 adapted from the method used by Boudah et al. Solvent B was varied as follows: 0min: 2%, 2
477 min: 2%, 10 min: 5%, 16 min: 35%, 20 min: 100% and 24 min: 100%. The column was then
478 equilibrated for 6 min at the initial conditions before the next sample was analysed. The
479 volume of injection was 5µL. For LTQ-Orbitrap High-resolution experiments were performed
480 with Vanquish HPLC system coupled to an LTQ Orbitrap Velos mass spectrometer (Thermo
481 Fisher Scientific, Waltham, MA, USA) equipped with a heated electrospray ionization probe.
482 MS analyses were performed in positive FTMS mode at a resolution of 60 000 (at 400 m/z) in
483 full-scan mode, with the following source parameters: the capillary temperature was 275 °C,
484 the source heater temperature, 250 °C, the sheath gas flow rate, 45 a.u. (arbitrary unit), the

485 auxiliary gas flow rate, 20 a.u., the S-Lens RF level, 40 %, and the source voltage, 5 kV.
486 Metabolites were determined by extracting the exact mass with a tolerance of 5 ppm.
487 Combined analysis was performed using MetaboAnalyst v6.0.
488
489 **dNTPs quantification**
490 $4x10^6$ CD4 T cells activated in RPMI or HPLM for 4 days were washed with cold PBS then lysed
491 in ice cold 65% methanol, vortexed vigorously and incubated at 95°C for 3min. After cooling
492 down the samples on ice for 1 min, they were centrifuged at 14 000rpm for 3 min and the
493 methanol supernatant was collected into a new tube, dried with a Speedvac and stored at
494 -80°C. The extracted dNTP samples were analyzed by the RT-based primer extension dNTP
495 assay[25]. Briefly, the dNTP samples were used for each 20 μl single nucleotide incorporation
496 primer extension reaction by HIV-1 RT. The dNTP levels in each sample were determined
497 within the linear ranges of the dNTP incorporation (2~32% primer extension), and the primer
498 extension levels in each dNTP sample from a known number of cells were converted into dNTP
499 quantities (pmol) per $1x10^6$ cells.
500
501 **References**

502 1. Global HIV & AIDS statistics — Fact sheet | UNAIDS. Accessed August 7, 2025.
503 https://www.unaids.org/en/resources/fact-sheet
504 2. Fauci AS, Lane HC. Four Decades of HIV/AIDS — Much Accomplished, Much to Do. *New*
505 *England Journal of Medicine*. 2020;383(1):1-4. doi:10.1056/NEJMp1916753
506 3. Hargrave A, Mustafa AS, Hanif A, Tunio JH, Hanif SNM. Current Status of HIV-1 Vaccines.
507 *Vaccines (Basel)*. 2021;9(9). doi:10.3390/vaccines9091026
508 4. Shehata HM, Murphy AJ, Lee M kit S, et al. Sugar or fat? - Metabolic requirements for
509 immunity to viral infections. *Front Immunol*. 2017;8(OCT):1311.
510 doi:10.3389/fimmu.2017.01311
511 5. Williamson MK, Coombes N, Juszczak F, et al. Upregulation of glucose uptake and
512 hexokinase activity of primary human CD4+ T cells in response to infection with HIV-1.
513 *Viruses*. 2018;10(3). doi:10.3390/v10030114
514 6. Hegedus A, Kavanagh Williamson M, Huthoff H. HIV-1 pathogenicity and virion
515 production are dependent on the metabolic phenotype of activated CD4+ T cells.
516 *Retrovirology*. 2014;11(1). doi:10.1186/s12977-014-0098-4
517 7. Loisel-Meyer S, Swainson L, Craveiro M, et al. Glut1-mediated glucose transport
518 regulates HIV infection. *Proceedings of the National Academy of Sciences*. Published
519 online 2011. doi:10.1073/pnas.1121427109
520 8. Palmer CS, Duette GA, Wagner MCE, et al. Metabolically active CD4+ T cells expressing
521 Glut1 and OX40 preferentially harbor HIV during in vitro infection. *FEBS Lett*.
522 2017;591(20):3319-3332. doi:10.1002/1873-3468.12843
523 9. Palmer CS, Ostrowski M, Gouillou M, et al. Increased glucose metabolic activity is
524 associated with CD4+ T-cell activation and depletion during chronic HIV infection. *AIDS*.
525 2014;28(3):297-309. doi:10.1097/qad.0000000000000128

526 10. Valle-Casuso JC, Angin M, Volant S, et al. Cellular metabolism is a major determinant of
527 HIV-1 reservoir seeding in CD4+ T cells and offers an opportunity to tackle infection. *Cell*
528 *Metab*. 2019;29(3):611-626 e615. doi:10.1016/j.cmet.2018.11.015
529 11. Clerc I, Abba Moussa D, Vahlas Z, et al. Entry of glucose- and glutamine-derived carbons
530 into the citric acid cycle supports early steps of HIV-1 infection in CD4 T cells. *Nat*
531 *Metab*. 2019;1(7):717-730. doi:10.1038/s42255-019-0084-1
532 12. Lagziel S, Gottlieb E, Shlomi T. Mind your media. *Nat Metab.Nature Research*.
533 2020;2(12):1369-1372. doi:10.1038/s42255-020-00299-y
534 13. Cantor JR, Abu-Remaileh M, Kanarek N, et al. Physiologic Medium Rewires Cellular
535 Metabolism and Reveals Uric Acid as an Endogenous Inhibitor of UMP Synthase. *Cell*.
536 2017;169(2):258-272.e17. doi:10.1016/j.cell.2017.03.023
537 14. Leney-Greene MA, Boddapati AK, Su HC, Cantor JR, Lenardo MJ. Human Plasma-like
538 Medium Improves T Lymphocyte Activation. *iScience*. 2020;23(1).
539 doi:10.1016/j.isci.2019.100759
540 15. Sáez-Cirión A, Sereti I. Immunometabolism and HIV-1 pathogenesis: food for thought.
541 *Nature Reviews Immunology 2020 21:1*. 2020;21(1):5-19. doi:10.1038/S41577-020-
542 0381-7
543 16. Boulay A, Quevarec E, Malet I, et al. A new class of capsid-targeting inhibitors that
544 specifically block HIV-1 nuclear import. *EMBO Mol Med*. 2024;16(11):2918-2945.
545 doi:10.1038/S44321-024-00143-W
546 17. Cavrois M, De Noronha C, Greene WC. A sensitive and specific enzyme-based assay
547 detecting HIV-1 virion fusion in primary T lymphocytes. *Nature Biotechnology 2002*
548 *20:11*. 2002;20(11):1151-1154. doi:10.1038/nbt745
549 18. Jochmann R, Thurau M, Jung S, et al. O-Linked N -Acetylglucosaminylation of Sp1 Inhibits
550 the Human Immunodeficiency Virus Type 1 Promoter . *J Virol*. 2009;83(8):3704-3718.
551 doi:10.1128/jvi.01384-08
552 19. Wang W, Nie J, Prochnow C, et al. A systematic study of the N-glycosylation sites of HIV-
553 1 envelope protein on infectivity and antibody-mediated neutralization. *Retrovirology*.
554 2013;10(1). doi:10.1186/1742-4690-10-14
555 20. Shytaj IL, Procopio FA, Tarek M, et al. Glycolysis downregulation is a hallmark of HIV-1
556 latency and sensitizes infected cells to oxidative stress. *EMBO Mol Med*.
557 2021;13(8):e13901. doi:10.15252/EMMM.202013901
558 21. Guo H, Wang Q, Ghneim K, et al. Multi-omics analyses reveal that HIV-1 alters CD4+ T
559 cell immunometabolism to fuel virus replication. *Nat Immunol*. 2021;22(4):423-433.
560 doi:10.1038/s41590-021-00898-1
561 22. Zhou YH, Sun L, Chen J, et al. Tryptophan metabolism activates aryl hydrocarbon
562 receptor-mediated pathway to promote HIV-1 infection and reactivation. *mBio*.
563 2019;10(6). doi:10.1128/MBIO.02591-19/
564 23. Harms M, Smith N, Han M, et al. Spermine and spermidine bind CXCR4 and inhibit
565 CXCR4- but not CCR5-tropic HIV-1 infection. *Sci Adv*. 2023;9(27):eadf8251.
566 doi:10.1126/SCIADV.ADF8251

24. Diamond TL, Roshal M, Jamburuthugoda VK, et al. Macrophage tropism of HIV-1 depends on efficient cellular dNTP utilization by reverse transcriptase. *J Biol Chem*. 2004;279(49):51545-51553. doi:10.1074/jbc.m408573200

Acknowledgments

The authors thank Lucile Espert and Caroline Goujon for sharing reagents and advice, Nathalie Arhel for sharing the HIV-1 patients' strains, and all team members for technical help and advice. This work was supported by the French AIDS National Research Agency ANRS (ECTZ134139 to J.-L. B.), the U.S. National Institute of Health NIH (R01 AI136581 and R01 AI162633 to B. K.) and used METABOHUB project funded by the program Investments for the Future of the French National Agency for Research (N. L.-L. and F.B.; ANR 11-INBS-0010). L.C. was supported by the French AIDS National Research Agency ANRS (ECTZ134113) then by CNRS, A.L. was supported by the French Sidaction (#12619 and #13564), A.B. was supported by an ANRS grant attributed to F.P.B. (ECTZ192763), A.T. was supported by a French Sidaction grant attributed to L.C. (#20224), L.B. is supported by CNRS and F.P.B. and J.-L.B. by Inserm.

Competing interests

Authors declare that they have no competing interests.

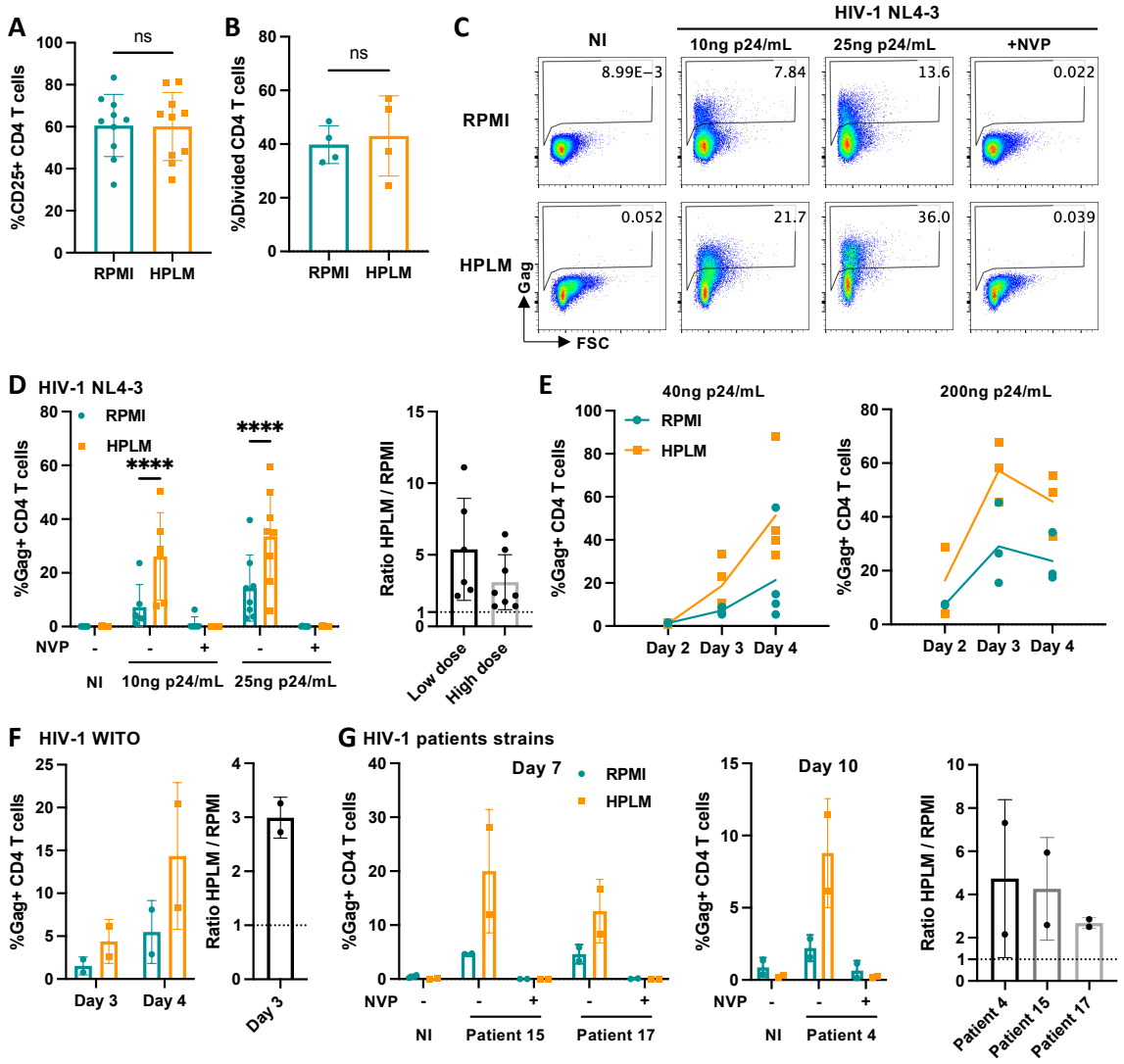

585

586 **Figure 1: Human plasma-like metabolic environment potentiates HIV-1 replication in**
587 **primary activated CD4 T cells.** Primary CD4 T cells activated in RPMI or in HPLM for 4 days
588 were infected with the indicated strains of HIV-1.
589 **A-B.** At day 4 (**A**) or 5 (**B**) post-activation, flow cytometry analysis of the CD25 activation
590 marker (**A**) and cell proliferation (**B**).
591 **C-E.** Cells were infected with the indicated doses of HIV-1 NL4-3 virus in the presence or
592 absence of the RT inhibitor nevirapine (NVP) as a control. Flow cytometry analysis of the HIV-
593 1 Gag expression at 4 days post-infection (dpi) (**C**, representative donor; **D**, pool) and over
594 time (**E**). NI: non-infected. Raw data (**D**, left) and fold changes in HPLM vs RPMI (**D**, right).
595 **F-G.** Cells were infected with 900ng p24/mL of the transmitted-founder HIV-1 WITO (**F**) or
596 primary isolates from HIV-1 infected patients using the highest possible doses: patient 15:
597 3,3ng p24/mL, patient 17: 23,5ng p24/mL, patient 4: 2,9ng p24/mL (**G**). Flow cytometry
598 analysis of the HIV-1 Gag expression at the indicated dpi. Raw data (left) and fold changes in
599 HPLM vs RPMI (right).
600 Data show mean±SD of n=10 (**A**), 3 or 4 (**B, E**), at least 6 (**D**) or 2 (**F**, **G**) donors. Statistical
601 analyses: (**A-B**) Mann-Whitney test; (**D**) 2-way ANOVA followed by Sidak's multiple
602 comparison test. ns: non-significant; ****: $p<0.0001$

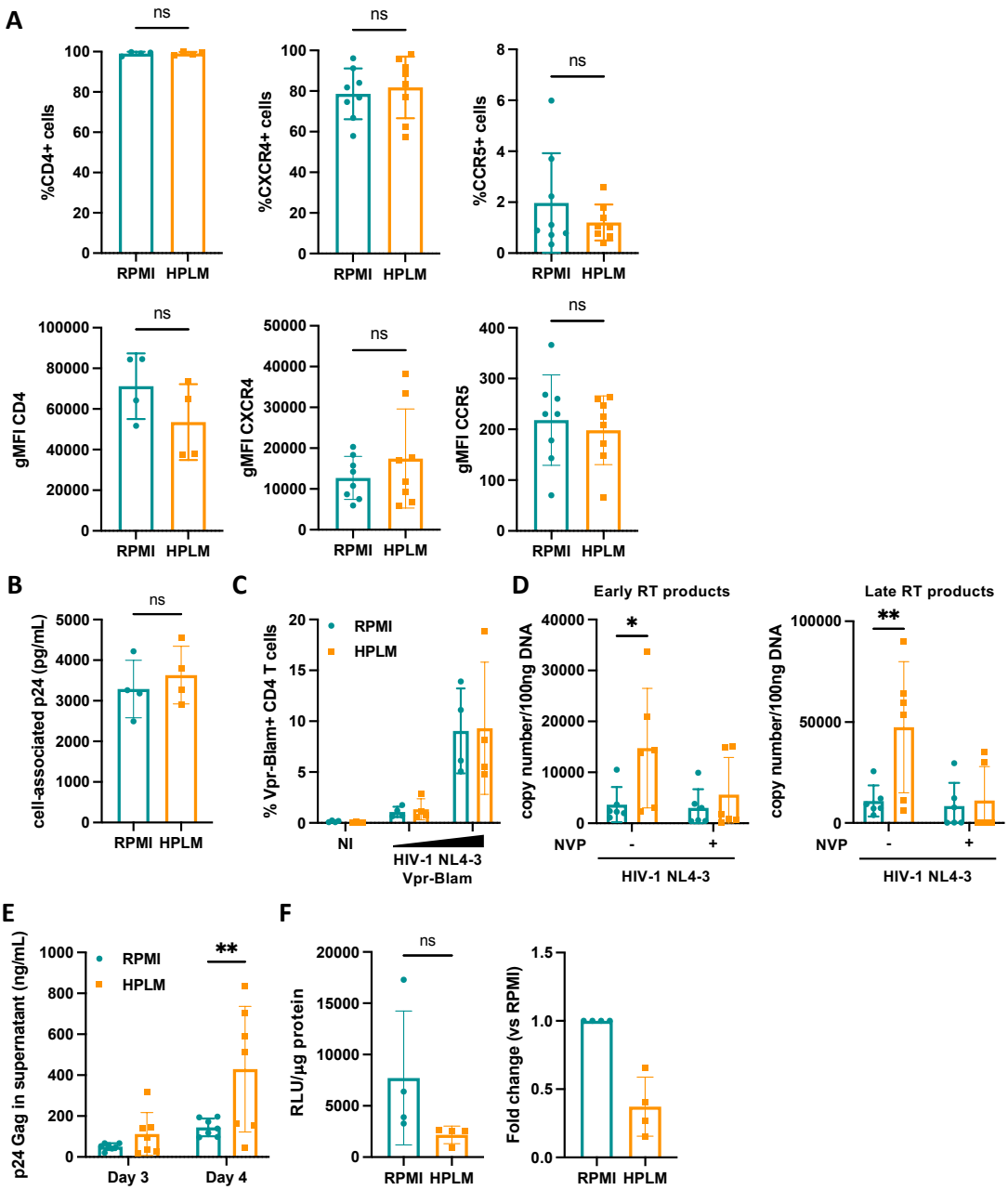

Figure 2: HPLM enhances HIV-1 reverse transcription. Primary CD4 T cells were activated in HPLM or RPMI and infected with the indicated viruses.

A. Flow cytometry analysis of the HIV-1 receptor CD4 and co-receptors CXCR4 and CCR5 at day 4 post-activation. Percentage of positive cells (upper panels) and geometric mean fluorescence intensity (gMFI) (lower panels).

B. Cells were placed at 4°C and incubated with 200ng p24/mL HIV-1 NL4-3 for 30min. After extensive washes, the cell-associated virus was quantified by HIV-1 p24 Gag ELISA.

C. Cells were infected for 2h with 2 doses of HIV-1 NL4-3 Vpr-Blam virus. Flow cytometry analysis of cells where viral fusion occurred using the Vpr-Blam assay. NI: non-infected.

D. Cells were infected for 2h with 200ng p24/mL DNase treated HIV-1 NL4-3 in the presence or absence of NVP (RT inhibitor) and incubated for 18h before DNA extraction. qPCR for the early and late RT products was performed on normalised quantities of cellular DNA.

616 **E-F.** Cells were infected with 40ng p24/mL HIV-1 NL4-3 for 2h, extensively washed and further
617 incubated. At 3 and 4 dpi, supernatants were collected. The amount of released virus particles
618 was quantified using anti-p24 ELISA (**E**) and their infectivity at 4 dpi was assessed by infecting
619 TZM-bl reporter cells with 5ng p24 of each supernatant (**F**). Raw data (**F**, left) and fold changes
620 in HPLM vs RPMI (**F**, right).
621 Data show mean±SD of n=at least 4 donors. Statistical analyses: Wilcoxon tests (**A, B, F**) or 2-
622 way ANOVA followed by Sidak's multiple comparison test (**D, E**). ns: non-significant. *: $p<0.05$;
623 **: $p<0.01$.

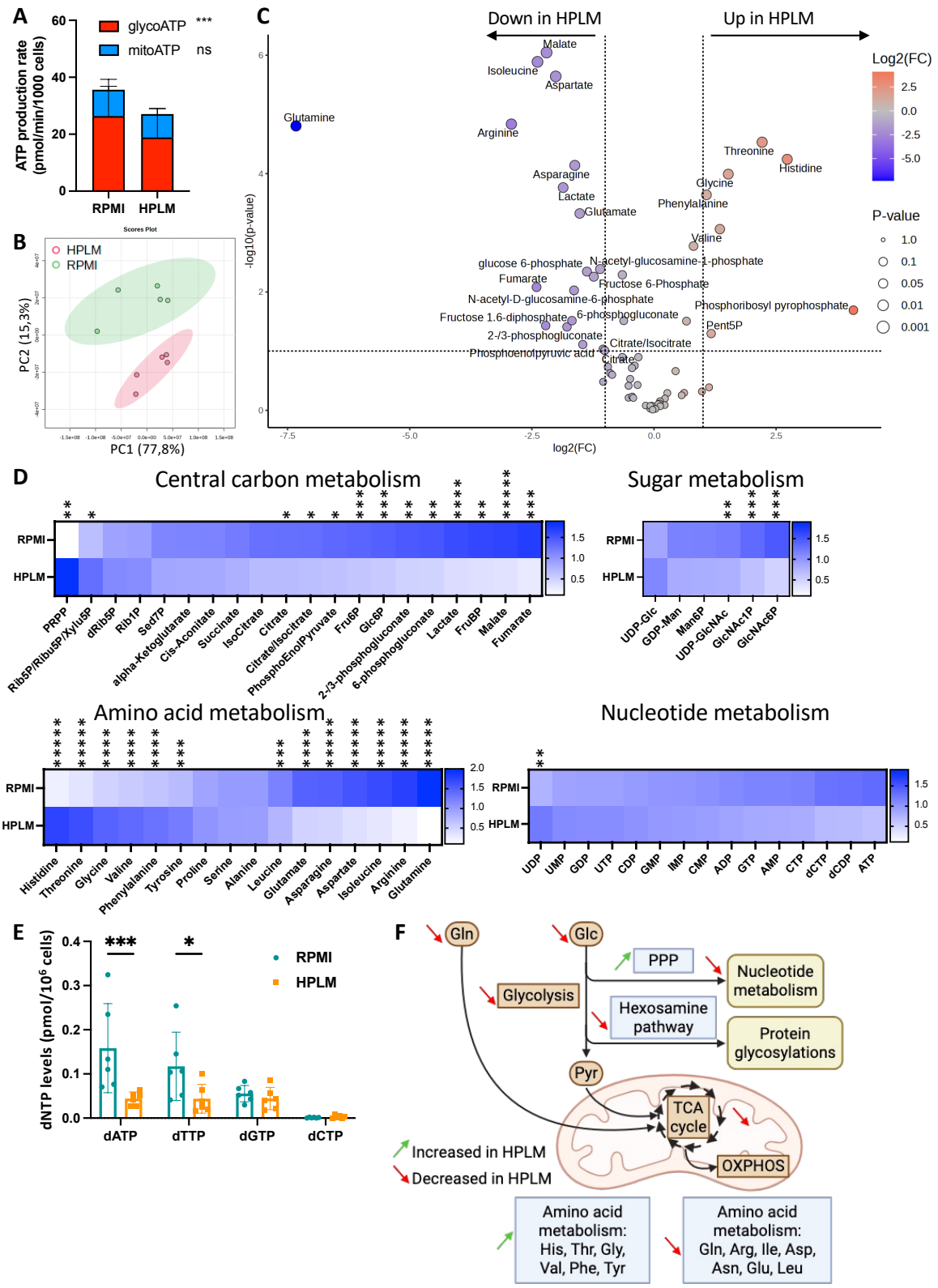

Figure 3: HPLM affects cellular metabolism of primary activated CD4 T cells. General metabolism of primary CD4 T cells activated in HPLM or RPMI was assessed.

A. Seahorse analysis showing ATP production rate in live cells, including individual contribution of glycolysis (GlycoATP) and OXPHOS (mitoATP).

B-D. Metabolomics analysis of activated cells from 5 donors by mass spectrometry. PCA analysis comparing the two conditions (**B**). Volcano plot highlighting metabolites with both

631 fold change >2 and p-value <0.1 (**C**). Heatmaps showing changes for each identified metabolite
632 separated into the main metabolic pathways (**D**).
633 **E.** Specific dNTPs quantification in activated cells.
634 **F.** Schematic representation of the metabolic pathways affected by HPLM (Created in
635 BioRender).
636 Data show mean±SD of n=6 (**A, E**) donors. Statistical analysis: 2-way ANOVA followed by
637 Sidak's multiple comparisons test (**A, E**), or using MetaboAnalyst (**B-D**). ns: non-significant; *:
638 p<0.1; **: p<0.5; ***: p<0.01; ****: p<0.001; *****: p<0.0001.

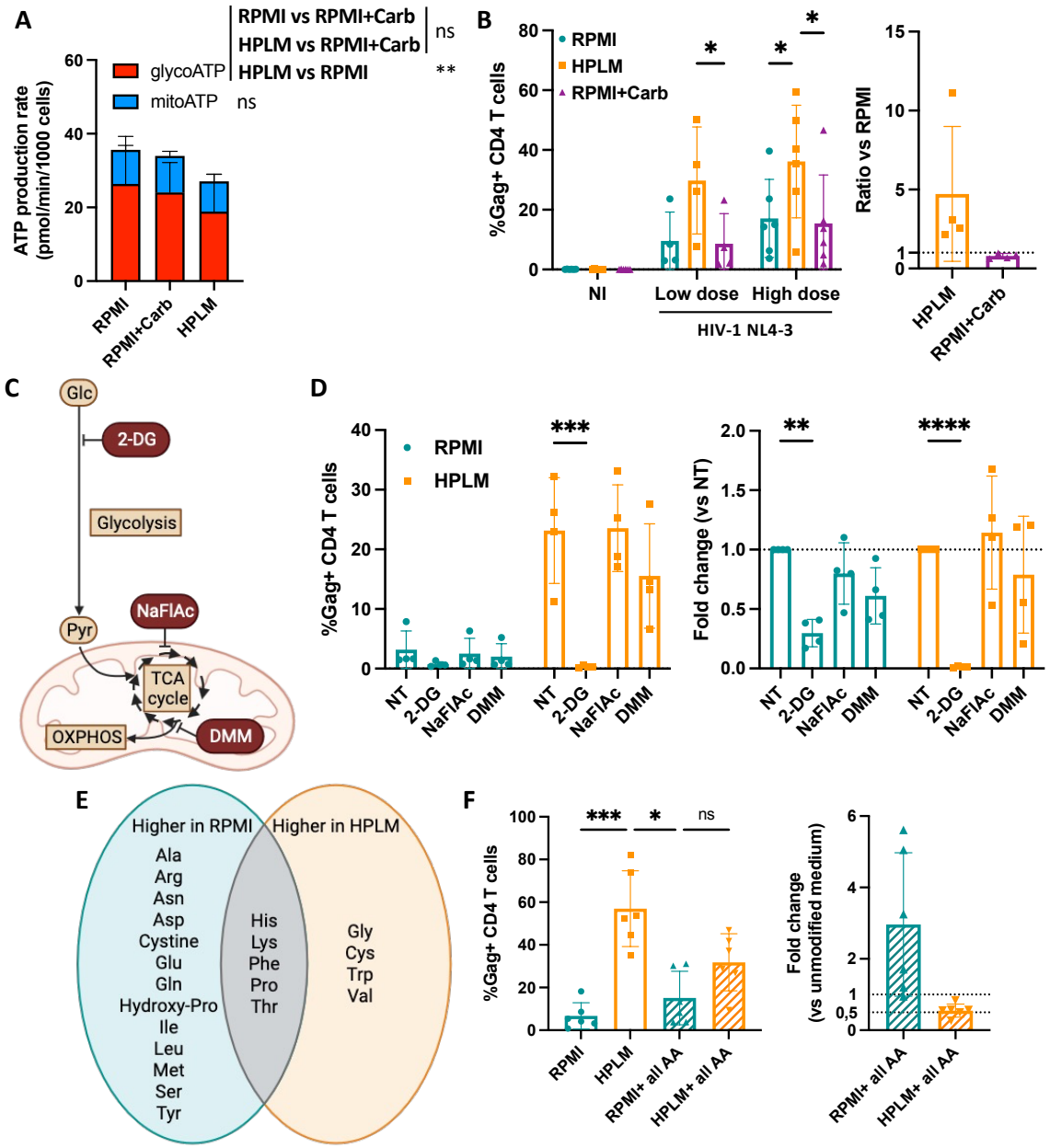

Figure 4: HPLM enhances HIV-1 infection by providing an optimal amino acid balance.

A-B. Primary CD4 T cells were activated in various media: HPLM, RPMI or RPMI with adjusted concentrations of glucose and glutamine to match the HPLM (RPMI+Carb). **A**. Seahorse analysis showing ATP production rate in live cells, including individual contribution of glycolysis (GlycoATP) and OXPHOS (mitoATP). **B**. Cells were infected as in Fig 1C. Flow cytometry analysis of the HIV-1 Gag expression at 4 dpi. NI: non-infected. Raw data (left) and fold changes in HPLM or RPMI+Carb vs RPMI (right).

C-D. Cells activated in RPMI or HPLM were infected with 25ng p24/mL HIV-1 NL4-3 in the presence of metabolic inhibitors. **C**. Schematic representation of the energy metabolic pathways targeted by the inhibitors used (Created in BioRender). **D**. Flow cytometry analysis of the HIV-1 Gag expression at 4 dpi. Raw data (left) and fold change compared to the non-treated condition (NT) (right).

652 **E-F.** Cells were activated in various media: RPMI, HPLM, RPMI with adjusted concentrations of
653 amino acids (RPMI+all AA) or HPLM with adjusted concentrations of amino acids (HPLM+all
654 AA). **E**. Schematic representation of the differences in levels of amino acids in the RPMI and
655 HPLM media. Amino acids higher in RPMI were adjusted in HPLM and vice versa. **F**. Flow
656 cytometry analysis of the HIV-1 Gag expression at 4 dpi with 40ng p24/mL. Raw data (left) and
657 fold change of adjusted media with corresponding unmodified medium (right).
658 Data show mean±SD of n= at least 4 (**A, B, D**) or 6 (**E-F**) donors. Statistical analysis: 2-way
659 ANOVA followed by Tukey's multiple comparisons test (**B**) or Dunnett's multiple comparisons
660 test (**D**); Friedman test followed by Dunn's multiple comparisons test (**F**). ns: non-significant;
661 *: $p<0.05$; **: $p<0.01$; ***: $p<0.001$; ****: $p<0.0001$.